

Civil Engineering Journal

(E-ISSN: 2476-3055; ISSN: 2676-6957)

Vol. 11, No. 09, September, 2025



A Procedure for Nonlinear Analysis of Laterally Loaded Single Piles and Pile Groups

Basuony M. El-Garhy ¹*o, Turki S. Alahmari ¹o, Ahmed M. Abdel Galil ²o

¹ Department of Civil Engineering, University of Tabuk, Tabuk 71491, Saudi Arabia.

Received 29 May 2025; Revised 21 August 2025; Accepted 26 August 2025; Published 01 September 2025

Abstract

This research introduces an analytical procedure for simulating the nonlinear behavior of single piles and pile groups under lateral loads in multi-layered, heterogeneous soil. The methodology combines the finite element method, the p-y technique, and the p-multiplier concept. Duncan and Chang's hyperbolic equation, characterized by three parameters, was employed to represent the soil reaction for sand and clay soils. A newly proposed equation to derive p-multipliers as a function of a pile's location and spacing within a pile group. Its predictions show satisfactory agreement with those from existing methods. The procedure was implemented in a computer program to enable rapid and accurate computation. The proposed program validation involved comprehensive comparisons against results from field load tests and sophisticated 3D finite element analyses. These comparisons confirm that the developed program is both reliable and efficient, making it well-suited for preliminary design stages. A subsequent parametric study on a single pile revealed that replacing soft upper clay with a compacted sand layer significantly decreases lateral deflection and bending moment. For the cases examined, an optimal compacted layer thickness of three pile diameters and a stiffness 5.6 times that of the native soft clay were identified.

Keywords: Laterally Loaded Single Pile; Laterally Loaded Pile Groups; P-Y Equation; P-Multiplier; Finite Element Method; Compacted Sand Layer; Soft Clay.

1. Introduction

Piles are foundational elements employed to carry both vertical and horizontal loading. Horizontal loads may be induced by seismic activity, wind, and soil pressure. Analyzing of piles under lateral loads constitutes a fully three-dimensional and highly nonlinear problem of significant complexity. To address this challenge, researchers frequently employ simplifications to develop solution algorithms that are more practical to implement. The approaches currently available to analyze piles under lateral loads range from complex techniques such as nonlinear 2D or 3D finite element analysis [1-4] to simplified approaches such as those based on the elasticity theory [5], the subgrade reaction analysis [6], the p-y technique [7-13], and the strain wedge, SW, approach [14-16].

The p-y technique, grounded in the Winkler model, is the common adopted practical method for analyzing laterally loaded piles among practicing engineers [13, 17]. This technique characterizes soil response through depth-specific, nonlinear p-y curves, whose properties are a function of soil type. Its prevalence is reflected in its incorporation into various design codes (e.g., [18, 19]) and commercial software packages like LPILE [9].

The original p-y curves for sand and clay soils, above and below the groundwater level, has been derived by back-calibrating data from field loading tests performed on piles whose diameters varied from 0.32 m to 0.61 m [7, 8, 20]. Therefore, these traditional p-y methods are best suited for piles that has diameters less than 0.61 m [21, 22]. Their

^{*} Corresponding author: belgarhy@ut.edu.sa





© 2025 by the authors. Licensee C.E.J, Tehran, Iran. This article is an open access article distributed under the terms and conditions of the Creative Commons Attribution (CC-BY) license (http://creativecommons.org/licenses/by/4.0/).

² Department of Civil Engineering, Menoufia University, Shebin El-Koom, Egypt.

application to larger-diameter piles requires specific adjustments to account for size effects [23-25]. Another recognized limitation of conventional p-y curve formulations is their excessively high initial tangent stiffness, which can lead to unrealistic modeling of soil-pile interaction, as noted by several researchers [26-29].

The experimentally derived p-y curves [30] were represented using the hyperbolic equation proposed by Kondner [31], which widely adopted in recent studies to represent p-y behavior in cohesionless soils [32-37]. Furthermore, Liang et al. [38] applied the same formulation to clay soils based on insights from 3D Finite Element Analysis (3D FEA). More recently, Alver & Eseller-Bayat [12] introduced a modified hyperbolic equation to characterize p-y curves for sand soil, informed by 3D FEA results. This enhanced equation incorporates four key parameters (i.e., initial tangent stiffness, limiting soil resistance, and two parameters describe the degree of nonlinear).

The behavior of a pile embedded in a group under horizontal loads is markedly differs from that of a solitary pile. Furthermore, the performance of any given pile in a group is influenced by its specific location (e.g., first row or second row) and its spacing to adjacent piles. These so-called group effects are commonly addressed employing the p-multiplier concept [39], which has been broadly adopted [36-43]. While many methodologies for calculating p-multiplier values, based on field tests of single piles and/or pile groups, are documented in the literature [35-39], their results frequently conflict, demonstrating a lack of consensus even when founded on full-scale data. Consequently, a definitive requirement remains for an uncomplicated and robust formula to accurately ascertain the p-multiplier.

This paper outlines a streamlined methodology for the nonlinear evaluation of laterally loaded piles in stratified soil deposits. The framework integrates the method of finite element (FEM) with the p-y technique and incorporates the p-multiplier concept. Soil resistance for both clays and sands is modeled via a hyperbolic relationship, following the Duncan & Chang [44] formulation. Additionally, a novel predictive equation for determining the p-multiplier is presented. This analytical approach has been encoded into a dedicated software application to facilitate efficient and precise computations.

The reliability of the developed program was assessed by benchmarking its predictions against both sophisticated 3D FEA and field loading tests. These evaluations involved single piles of varying diameters and multi-pile groups. Furthermore, the application was employed to investigate how replacing a surface layer of soft clay with compacted sand affects the response of a single pile that loaded laterally. Explanation of the analytical methodology is detailed in the following section, which precedes the validation of the program's results. The document concludes with a presentation of findings from a parametric analysis and the key conclusions drawn from the study.

2. Analysis Procedure

Figure 1 provides a definition sketch of a pile embedded within a stratified soil profile. The analyzed pile, characterized by a diameter D and a length L, experiences a constant axial force P_z concurrently with a lateral head load comprising force P and/or moment M. The properties of each distinct soil stratum, including its thickness H_i , effective unit weight γ'_i , angle of internal friction ϕ_i , and Poisson's ratio v_{si} are defined. The elasticity modulus of the soil layers may be constant, vary linearly, or change nonlinearly with depth, as depicted in Figure 1 and calculated from Equation 1.

$$E_{szi} = E_{soi} + R_i z_i^{n_i} \tag{1}$$

where E_{szi} is the elasticity modulus at depth z from layer surface, E_{soi} is the elasticity modulus at the layer surface, R_i is the change's rate with depth, n_i is the exponent, and i is the layer number. For cohesive soil layers, a similar formulation to Equation 1 is employed to represent the change of soil cohesion with depth within each individual layer.

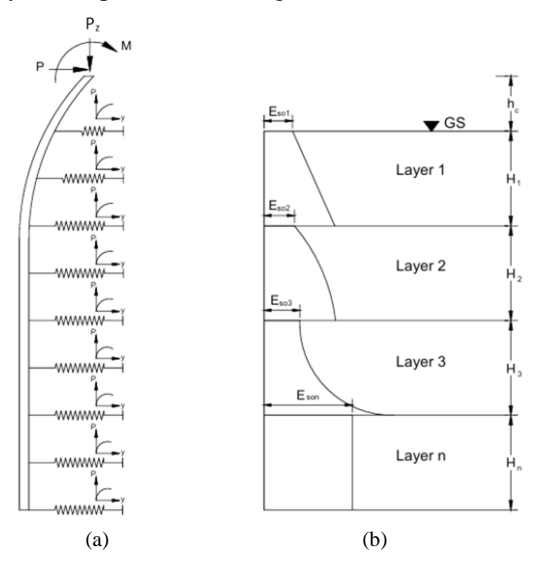


Figure 1. Schematic of the problem: (a) Modelling of a laterally loaded pile using nonlinear springs, (b) Multi-layered soil profile

The differential equation controls the bending of the laterally loaded pile subjected to a constant axial force, P_z , is as follows:

$$E_p I_p \frac{\partial^4 y}{\partial z^4} + P_z \frac{\partial^2 y}{\partial z^2} + k_h y = 0 \tag{2}$$

where E_p , I_p are the pile's elastic modulus and cross-sectional moment of inertia, respectively, E_pI_p is the pile's flexural stiffness, y is the displacement, z is the depth below the head of the pile, and k_h is the horizontal modulus of subgrade reaction.

The soil's resistance is simulated with a set of discrete, nonlinear p-y springs located at nodes along the pile shaft. In this study, the nonlinear response of soil resistance is simulated using the well-established hyperbolic equation of Duncan & Chang [44].

$$p = y \left(\frac{1}{k_{hi}} + \frac{y R_f}{P_H} \right)^{-1} \tag{3}$$

where p is the soil's resistance (kN/m); y is the displacement (m); k_{hi} is the initial tangent stiffness (kN/m^2) , P_u is the limiting soil resistance (kN/m), and R_f is a curve fitting constant governing nonlinearity.

This investigation employs the FEM to model the soil-pile system and compute the resulting internal pile forces alongside the corresponding soil reactions at nodal locations. The pile is subdivided into beam-column elements, capable of sustaining axial loads, which can have either uniform or variable lengths. The total count of these elements is determined by the number of segments within the soil strata plus any segments representing the unsupported pile segment above ground. At interface nodes between soil layers, the k_{hi} and P_u are averaged from the values at the adjacent nodes in the upper and lower layers. The solution is achieved through an iterative nonlinear analysis procedure designed to capture the progressive reduction in system stiffness as the load is applied in increments. This numerical method is implemented in a FORTRAN-based computer program named LLSPNL. For each load increment, the tangent stiffness, k_{ht} , of the p-y curve at each node is calculated by Equation 4 [45].

$$k_{ht} = k_{hi} \left(1 - \frac{R_f p}{P_u} \right)^2 \tag{4}$$

where the parameters in Equation 4 are as previously described.

Equation 3 is controlled by three parameters (i.e., k_{hi} , P_u , and R_f) whose estimation is detailed in the subsequent sections.

2.1. The Initial Tangent Stiffness

The parameter k_{hi} is typically derived from the E_s of the soil. Following a comparative analysis of six existing equations, Yu et al. [46] recommended that the expression developed by Liang et al. [38] was the most accurate. Consequently, the present study adopts Liang et al.'s equation (Equation 5) to estimate k_{hi} .

$$k_{hi} = 0.943 \left(\frac{1}{v_S^{0.078}}\right) \left(\frac{D}{D_{ref}}\right) \left(\frac{E_S^{1.036}}{E_p^{0.031}}\right) \left(\frac{z}{z_{ref}}\right)^{0.016} \tag{5}$$

where D_{ref} and z_{ref} are reference values for diameter and depth z below the ground, respectively, both set to 1.0. All other parameters in Equation 5 retain their previously stated definitions.

A key advantage of Equation 5 is its comprehensive incorporation of the primary parameters influencing laterally loaded pile behavior (i.e., soil elastic properties, pile modulus and diameter, and depth) into the calculation of k_{hi} . Furthermore, it successfully mitigates the previously overlooked diameter effect [20] inherent in earlier p-y curve models.

The soil elasticity modulus can be obtained through laboratory testing or estimated via empirical correlations. For cohesive soils, E_s is commonly expressed as a function of undrained cohesion, c_u , with a typical E_s/c_u ratio ranging from 200 to 900 and an average of 500 [47]. For cohesionless soils, E_s is correlated with the SPT blow count (e.g., N_{60}) [47-51]. Appropriate values for the soil's Poisson's ratio may be selected from established sources such as Bowles [48].

2.2. Limiting Soil Resistance

The limiting soil resistance, P_u , for different soil types has been estimated by using a 3D model of soil's passive wedge in the side facing the direction of load [14-16, 38, 52]. For piles in clay, Jeong et al. [52] proposed Equation 6 for P_u .

$$P_u = (S_1 p_{max} + S_2 \tau_{max})D = (S_1 10c_u + S_2 2c_u)D$$
(6)

where p_{max} is the frontal pressure $(10c_u)$, τ_{max} is the maximum side shear resistance $(2c_u)$, S_1 and S_2 are cross-section shape factors. These shape factors for circular cross-section are 0.75 and 0.5, respectively, and both equal 1.0 for square cross-section [53].

For piles in sand, Zhang et al. [54] suggested Equation 7 to calculate P_u .

$$P_u = (S_3 p_{max} + S_4 \tau_{max}) D = \left(S_3 K_p^2 \gamma' z + S_4 K \gamma z t a n \delta \right) D \tag{7}$$

where K_p is the passive earth pressure coefficient, K is the earth pressure coefficient (varies from K_o to 1.75 [48]), K_o is the at-rest coefficient, Z is the depth, Y is the effective unit weight, S is the pile-soil friction angle ($S \cong 0.67\phi$ [48]), and S_0 and S_0 are shape factors. For a circular cross-section, the shape factors are 0.8 and 1.0; for a square cross-section, they are 1.0 and 2.0 [53].

2.3. Hyperbolic Curve Fitting Constant

The R_f constant describes the soil nonlinearity. Its value ranges from 0 (elastic-perfectly plastic behavior) to 1.0 (highly nonlinear behavior) [45].

2.4. Pile Group

The performance of a pile in a closely-spaced group that laterally loaded deviates from that of a solitary pile due to interactions among the piles. This group effects have been studied through full-scale and model load tests [39, 42, 55, 56]. A pile in the 1st row (i.e., leading row) behaves as a single pile, while piles in subsequent rows exhibit reduced lateral resistance and a softer load-displacement response. This reduction, known as the "shadowing effect," is caused by overlapping stress zones from the front piles. The shadowing effect diminishes with increased pile spacing and becomes negligible at a spacing-to-diameter ratio greater than six [57].

Brown et al. [39] developed the p-multiplier, f_m , from field load test results to model group effects. This technique scales the p-values from a solitary pile's p-y curve by the factor f_m to get the attenuated p-y reaction for a pile in a group, as illustrated in Figure 2. This study employs the following hyperbolic p-y curve equation for the group of piles, incorporating the p-multipliers concept [11].

$$p = y \left(\frac{1}{f_{m}k_{H}} + \frac{yR_{f}}{f_{m}R_{H}}\right)^{-1} \tag{8}$$

where f_m is the p-multiplier and the other parameters in Equation 8 are as defined earlier.

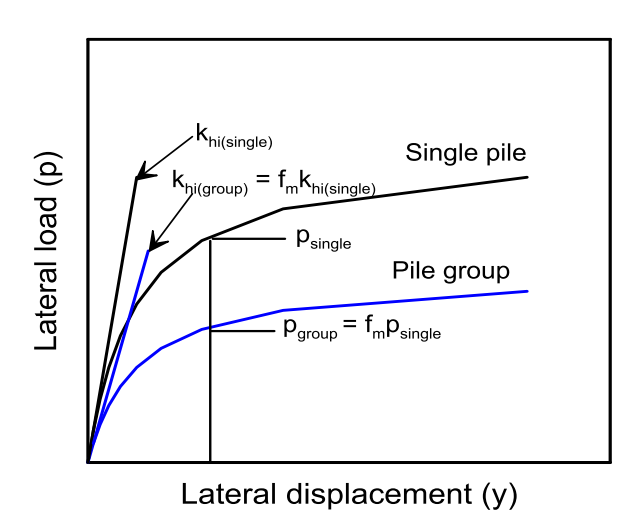


Figure 2. The p-multiplier concept of pile group

2.4.1. The p-Multiplier

The magnitude of the f_m varies according to the pile's location in the pile group (leading or trailing row), spacing between piles, and type of soil. For a group analysis, an average f_m value termed the Group Reduction Factor (GRF) is calculated across all rows [42, 58]. Recommended values for f_m from the technical literature are depicted in Table 1 [59].

Table 1. Recommendations for the values of the f_m

Reference	Soil type	Pile properties			f_m		
Kelerence	Son type	r ne properues	Lead row 2 nd row 3 rd row		Trailing rows	Last row	
[42]	Clayey silt	Driven steel pipe pile filled with concrete (D= 0.324 m)	0.60	0.40	0.40	-	-
[41]	Loose fine sand	Driven 0.72 m square prestressed concrete pile	0.80	0.70	0.30	0.30	-
[39]	Medium sand	Driven 0.272 m OD steel pipe pile filled with grout	0.80	0.40	0.30	-	-
	C1	D. 0072 OD . 1 . 1 . 1 . 11 . 11	0.70	0.60	0.50	-	-
[60]	Clay	Driven 0.272 m OD steel pipe pile filled with grout		0.50	0.40	-	-
[43]		Bored concrete shaft (D=1.5 m)	0.50	0.40	0.30	-	-
[43]		Driven 0.8-square prestressed concrete piles	0.90	0.70	0.50	0.40	-
[40]	Sand	Recommendation	0.80	0.40	0.30	0.20	0.30

In this research, the chart of Mokwa & Duncan [61] for the p-multiplier is transformed into an equation for simplicity and accuracy. The f_m value for a given row is defined by the following linear expression.

$$f_m = a + b(S/D) \tag{9}$$

where a, b are two constants' functions of the row number and the ratio S/D as shown in Table 2.

Table 2. constants of Equation 9 for each row

Row	Constants			
number	а	b		
1	0.64	0.06		
2	0.34	0.11		
3	0.10	0.15		
4+	0.04	0.16		

The two constants a and b are drawn as functions of row number, N_r , and can be reasonably calculated from the following two polynomials fitting equations with R^2 greater than 0.9968 and a residual sum of squares less than 0.0002.

$$a = 1.09 - 0.504N_r + 0.06N_r^2 \tag{10}$$

$$b = -0.015 + 0.084N_r - 0.01N_r^2 (11)$$

The f_m calculated from Equations 9 to 11 is considered equal to 1.0 for S/D ratio greater than or equal to 6. Based on comparisons with numerous methods, it is observed that Equation 9 calculated higher values for the f_m for the different rows. Consequently, the authors introduce a reduction factor, R_{f_m} , applied to the calculated f_m values as defined in Equation 12.

$$f_m = R_{f_m}[a + b(S/D)] \tag{12}$$

As detailed in Table 3, the reduction factor, R_{f_m} , depends on the row number and the soil type.

Table 3. The reduction factor (R_{f_m})

Soil type		Clay soil		Sandy soil
Row number	1st row (Leading row)	2nd row and subsequent trailing rows	1st row (Leading row)	2nd row and subsequent trailing rows
R_{f_m}	0.95	0.80	0.85	0.70

Table 4 compares the f_m values calculated from Equations 9 and 12 with those obtained by the FEMA P-751 [62] and AASHTO [19, 63] recommendations for a 4×4 pile group at various S/D ratios.

	FEMA I	P-751 [62] g	guidelines	AASI	HTO [19] gui	idelines		Equation 9)		Equation 12	2
Row No.	S/D		S/D		S/D		S/D					
	3	4	5	3	4	5	3	4	5	3	4	5
1	0.79	0.86	0.92	0.8	0.9	1.0	0.82	0.88	0.94	0.78	0.84	0.89
2	0.57	0.72	0.84	0.4	0.625	0.85	0.66	0.77	0.89	0.43	0.5	0.58
3	0.41	0.58	0.72	0.3	0.5	0.7	0.55	0.71	0.85	0.36	0.46	0.55
4+	0.41	0.58	0.72	0.3	0.5	0.7	0.52	0.68	0.83	0.34	0.44	0.54

Table 4. The f_m values obtained by Equations 9 and 12 and those obtained from other guidelines for 4×4 group of piles

As depicted in Table 4, Equation 12 predicted values of f_m comparable to those obtained from FEMA P-751 [62] guidelines and AASHTO [19] guidelines for 4×4 group of piles. Therefore, Equation 12 is selected for use in the present study.

3. Program Validation

The LLSPNL program was validated against 3D FEA and field measurements. The validation cases included individual piles and pile groups in variant soil profiles, including sand, clay, and multi-layered soils.

3.1. Comparison with 3D FEA

Gupta & Basu [64] performed a nonlinear 3D FEA using the ABAQUS software for two single piles, one embedded in clay soil and the other in sand soil. The two examples of single piles were solved by the proposed program for validation and verification.

3.1.1. Single Pile in Clay Soil

The first example is an RC pile of 1.0 diameter, 30 m length, and the E_p of 28 GPa. The pile is embedded in undrained clay with the E_s of 59.6 MPa and a Poission's ratio of 0.49. The applied lateral load was 2000 kN. In the present analysis, the c_u of the clay is considered 284.5 kN/ m^2 (i.e., equal to E_s /210). E_s is taken 1.0. Figures 3 and 4 illustrate the current results with 3D FEA results for the load-displacement at the head of the pile and the profile of lateral displacement with depth, respectively.

As illustrated in Figure 3, a generally good comparison is obtained. More specifically, at the early stages of lateral loads, the lateral displacements of the 3D FEA are slightly greater than the displacements obtained by the present method, whereas at the lateral load higher than 1.5 *MN*, the two methods generate the same lateral displacements. Figure 4 shows a strong correlation between the lateral displacement profiles from the current analysis and the 3D FEA, especially within the upper 5-meter depth.

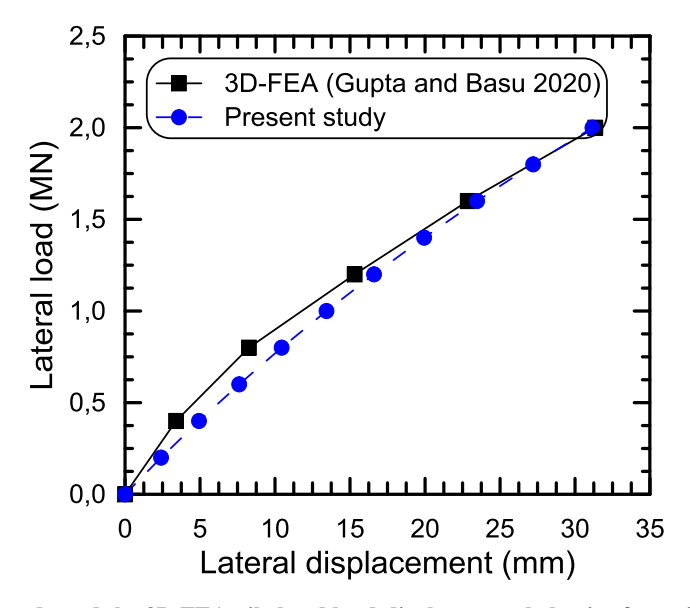


Figure 3. The present study and the 3D FEA pile head load-displacement behavior for a single pile in clayey soil

Vol. 11, No. 09, September, 2025

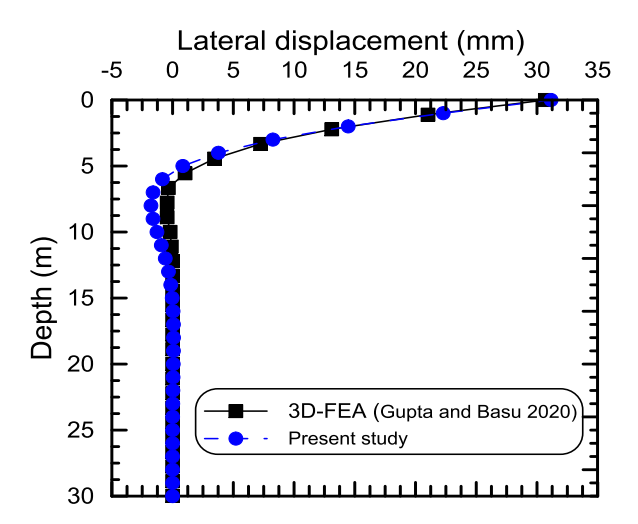


Figure 4. The present study and the 3D FEA lateral displacement profile along pile length for a single pile in clayey soil

3.1.2. Single Pile in Sand Soil

The analysis considers a reinforced concrete pile of a 0.9 m diameter and a 30 m long, installed in sand soil. The elastic modulus of the pile was 28 GPa. The properties of the sand are E_s of 80 MPa, a v_s of 0.25, and a ϕ of 38.5°, as per Bowles [48]. The pile was loaded at its head a force P of 1000 kN acting in conjunction with a 305 $kN \cdot m$ moment. R_f was considered 1.0. Figures 5 and 6 illustrate the current results with 3D FEA results for the load-displacement response and the profile of lateral displacement with depth, respectively. The close alignment between the present study and the 3D FEA validates the numerical model.

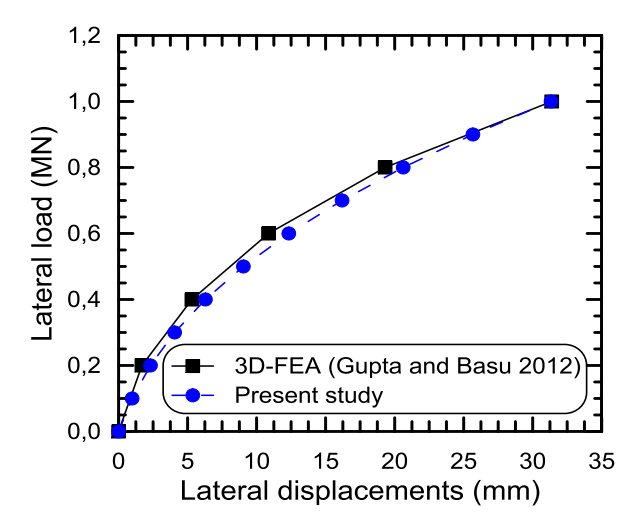


Figure 5. The present study and the 3D FEA pile head load-displacement behavior for a single pile in sandy soil

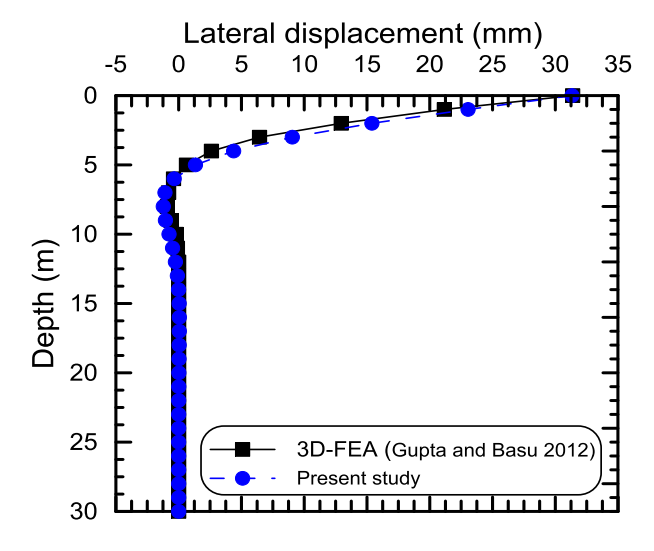


Figure 6. The present study and the 3D FEA lateral displacement profile along pile length for a single pile in clayey soil

3.2. Comparison with Full-Scale Loading Test

This segment provides a comprehensive validation of the developed program's output against data from field lateral loading tests conducted on piles (i.e., individual piles and pile groups) situated in diverse, stratified soil conditions. The case studies encompass piles with different diameters (i.e., 0.321 m to 1.0 m).

3.2.1. Comparisons of Single Piles

Field Test at Aliakmon River, Greece

Comodromos & Pitilakis [65] documented a field lateral loading test performed of on a 52 m long, 1.0 m diameter concrete pile at the Aliakmon River bridge site in Greece. The pile was installed in a 3-layer soil profile, their properties detailed in Table 5. For the present modelling, the v_s was taken 0.3 for all layers. The elastic moduli were defined as $E_s = 234c_u$ for soft clay and $E_s = 150c_u$ for hard clay. These E_s/c_u ratios are within the established range of 200 to 900 reported by Callanan [47] and Bowles [48]. The R_f was taken as 1.0.

Layer	T f!	Layer thickness	Soil properties				
No.	Type of soil	(m)	ϕ^o	$\gamma (kN/m^3)$	$c_u (kN/m^2)$		
1	Soft clay (CL)	0.0 - 36.0	0.0	20	5 – 50		
2	Hard clay (CL)	36.0 - 48.0	0.0	20	110		
3	Gravel (GW)	48.0 - 52.0	40	22	0.0		

Table 5. Properties of soil layers at Aliakmon River, Greece [65]

Figure 7 compares the lateral displacement from the present study with field measurements and 3D FEA (FLAC-3D) predictions for an applied force of 1200 kN. The current results closely align with the field measurements. Conversely, the 3D FEA outcomes align with the recorded displacements solely up to a load of approximately 0.4 MN, deviating to slightly lower values under higher loads.

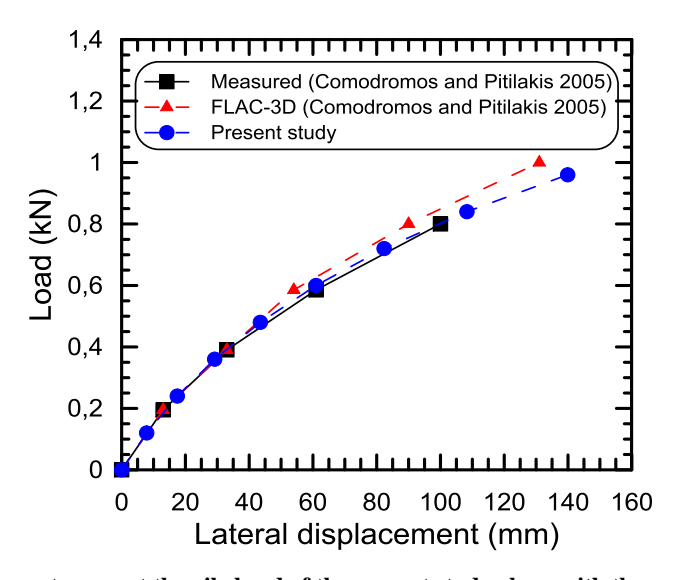


Figure 7. The load-displacement curve at the pile head of the present study along with those measured and predicted by FLAC-3D for a single pile at Aliakmon River, Greece

Field Test at Manor, Texas

A field load test performed on a 15.20 m length, 0.642 m outer diameter steel pipe pile ($E_pI_p=493.7~\mathrm{MN\cdot m^2}$) in Manor, Texas, was reported by Reese [66]. The pile, embedded in saturated, very stiff clay and laterally loaded by a 600 kN at 0.305 m above the ground. For modeling purposes, the soil profile was simplified into two-layer. Layer No. 1 (3.97 m thick) had an elastic modulus of 82,400 kPa, approximately 400 times the average c_u of 206 kPa. Layer No. 2 had an elastic modulus of 83,800 kPa, equivalent to $250c_u$. Poisson's ratio for the two-layer was considered 0.47, and R_f was considered 1.0. Figure 8 demonstrates a close correlation between the current prediction and the measured load-displacement behavior. While the initial predicted displacements are slightly elevated, the curves converge precisely at the peak load of 600 kN.

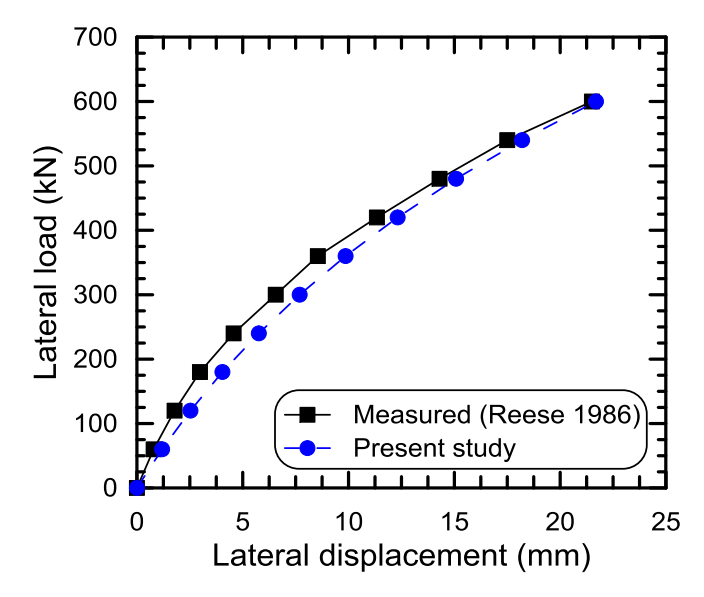


Figure 8. Measured and predicted lateral load-displacement curve of the present study at the pile head at Manor test site

Field Test at Lake Austin, Texas

A loading test conducted on a steel pile at the site of Lake Austin in Texas, USA, was summarized by Reese [66] based on original work by Matlock [20]. The test pile was of 12.8 m length, 0.321 m outer diameter, and a bending stiffness, $E_p I_p$, of 31.28 MPa. A lateral force was applied at the ground level. The soil was characterized as a lightly over-consolidated, fissured clay, possessing a shear strength of 38.3 kPa and a buoyant unit weight of 7.86 kN/m^3 . In the numerical modeling, the E_s of the clay was defined as 220 times its undrained shear strength [67, 68], while a v_s of 0.47 [48], and the R_f value of 1.0 were adopted. Figure 9 shows a close agreement between the predicted and measured load-displacement responses at the ground surface confirms the model's accuracy in simulating the pile's behavior.

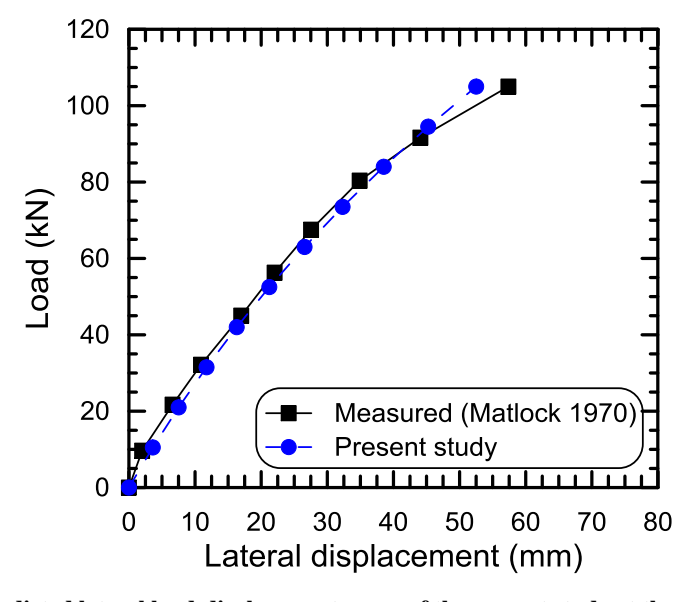


Figure 9. Measured and predicted lateral load-displacement curve of the present study at the pile head at the Lake Austin test site

Field Test at Sabine, Texas

After testing in Lake Austin, the same pile was used and installed at a Sabine, Texas site and laterally loaded 0.305 m above grade [20]. The slightly over-consolidated marine soft clay at this location had a cohesion of 14.40 kPa and an effective unit weight of 5.5 kN/m^3 .

In the present modeling an elastic modulus defined as $486c_u$ [67, 68], a Poisson's ratio of 0.47 [48], and R_f equal to 1.0 were adapted. The strong concordance between the predicted and experimental load-displacement curves in Figure 10 validates the program's capability to accurately represent pile behavior in soft clay.

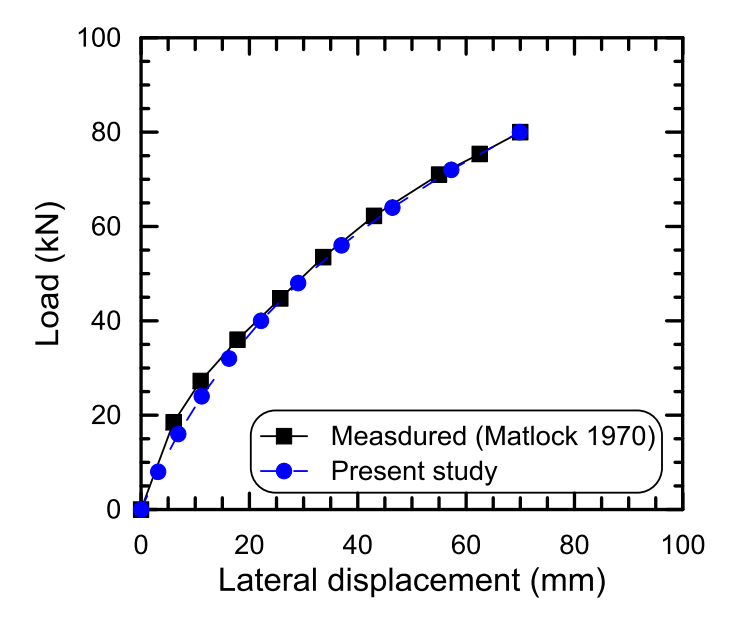


Figure 10. Measured and predicted lateral load-displacement curve of the present study at the pile head at Sabine test site

Field test at Treasure Island, California

A loading test conducted on a pipe pile, open ended, at the site of Treasure Island, California, was detailed by Rollins et al. [69]. The pile was of 11.5 m length, 0.324 outer diameter, and 0.305 inner diameter. To safeguard the instrumentation, steel angles were fastened along the sides of the pile aligned with the loading direction; this reinforcement increased its moment of inertia from an original $1.16 \times 10^{-4} \, m^4$ to $1.43 \times 10^{-4} \, m^4$ [65], yielding a composite bending stiffness, $E_p I_p$, was 28,600 kN·m². The load was acting laterally at a 0.69 m above the grade, reached a peak value of 113.5 kN. During testing, the GWT was recorded at a 0.5 m depth below the ground. The pile installed in a subsurface profile consisting of eight distinct layers. The geotechnical properties and stratigraphy for these layers are detailed in Table 6.

	Soil Layer	(1.11/.3)	(1 N / 2)	(10)	.,		1 (13)	1 (13)
No.	Thickness (m)	$-\gamma (kN/m^3)$	$c (kN/m^2)$	(ϕ^o)	N ₆₀	N ₅₅	$k_{hi} (kN/m^3)$	$k_{hi} (kN/m^3)$
1	0.0 - 0.51	19.5	0	39	10	10.9	60	33820.2
2	0.51 - 2.97	10.3	0	39	10	10.9	35.2	31662.0
3	2.97 - 3.99	10.3	0	37	10	10.9	29.8	31662.0
4	3.99 - 6.00	10.3	0	36	7	9.3	24.4	25399.2
5	6.00 - 7.49	10.3	0	35	7	7.6	21.7	25399.2
6	7.49 - 9.25	9.5	19.2	0	-	-	1.2	3840.0
7	9.25 – 10.16	10.3	0	34	2	2.2	19.0	10727.6
8	10.16 – 11.84	9.5	19.2	0	-	-	1.2	3840.0

Table 6. Properties of the soil stratums [65]

This analysis employs friction angles for the sand stratums that were adjusted by Bolton [70] and subsequently cited by Rollins et al. [69] (Table 6). The elastic modulus for each layer was derived from SPT (N_{60}) blow counts by averaging the values obtained from three separate equations (i.e., Equations 13 to 15) provided by Bowles [48]. For clay soil layers, the modulus of elasticity is taken as $200c_u$ according to Bowles [48]. The R_f was taken 0.85.

$$E_s = 500(N_{55} + 15) \tag{13}$$

$$E_s = 7000\sqrt{N_{55}} \tag{14}$$

$$E_s = 6000N_{55} \tag{15}$$

where $N_{55} = (60/55)N_{60}$ [53].

As illustrated in Figure 11, the close correlation between the predicted and experimental load-displacement behavior validates the program's capability to accurately simulate the lateral response of a single piles.

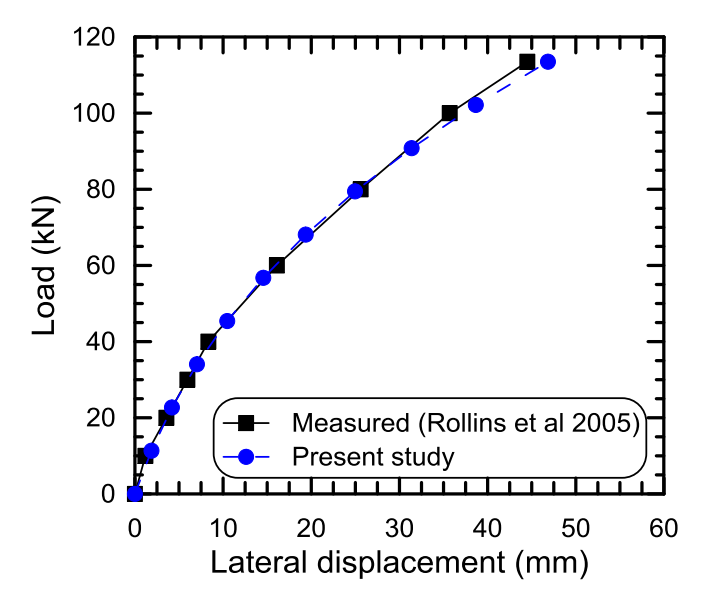


Figure 11. Measured and predicted lateral load-displacement curve of the present study at the pile head at Treasure Island test site

3.2.2. Comparisons of Pile Groups

Full-Scall Field Test on Pile Group in Sand

A loading test on a group of piles (i.e., 3×3) was documented by Rollins et al. [56]. The group had an S/D ratio of 3.3 in the two directions and was composed of piles similar to those employed in the prior test of the individual pile. Key differences in the group test configuration included a load application point elevated 0.86 m above grade and a significantly higher groundwater table, present at just 0.1 m below the surface. According to Rollins et al. [56], these altered hydrostatic and loading conditions preclude a reliable direct comparison between the isolated pile and group responses. To model the group's behavior, the soil parameters from Table 6 were adapted to reflect the elevated water table. Specifically, for the uppermost layer, the submerged unit weight was reduced to $10.3 \, kN/m^3$ and its elastic modulus was correspondingly set to $10.3 \, MPa$. Figure 12 depicts a comparison of the curves of load-displacement. It includes the predicted response for the single pile (simulated using the LPILE program by Rollins et al. [56] and replicated here using the group's modified soil properties for consistency) alongside the measured responses for the front and middle rows of the group. The close match between the computed and observed group pile curves confirms the model's proficiency in analyzing pile group interaction.

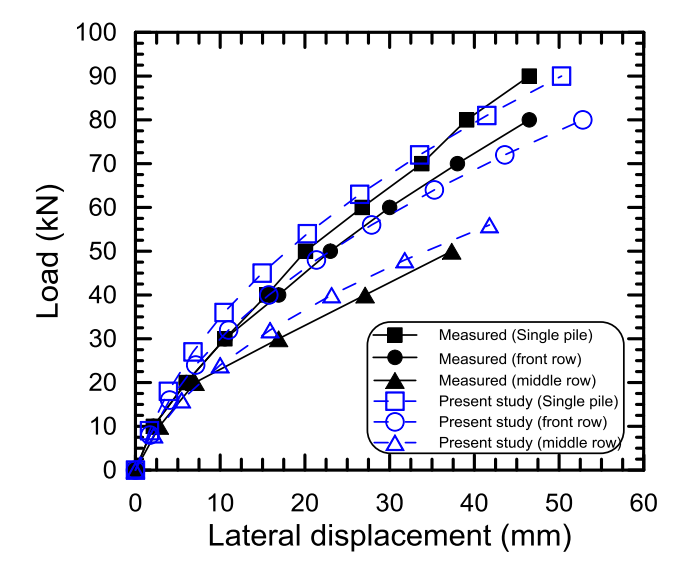


Figure 12. Measured and predicted lateral load-displacement curves at the pile head for the single pile, front row, and middle row at Treasure Island test site

The p-multipliers, f_m , computed in this analysis are 0.799 and 0.556 for the front and the middle rows, respectively. The results show minor variations from the values of 0.8 and 0.4 published by Rollins et al. [56]. The observed differences are primarily attributable to variations in the methods employed for generating p-y curves in the current model and the LPILE software.

Figure 13 illustrates the correlation between the computationally modeled and experimentally observed lateral load-displacement responses of the pile group. The simulation conducted in this study, which employed an average p-multiplier, f_m , of 0.612, correlates closely with the field data. Conversely, the application of the average f_m value of 0.533 documented by Rollins et al. [56] results in a conservative prediction that slightly overestimates the displacements observed in the field test.

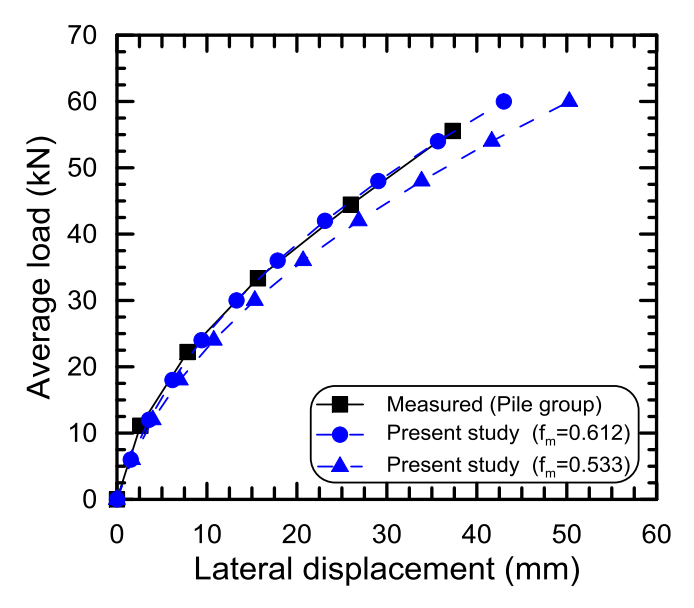


Figure 13. Measured and predicted lateral load-displacement responses for the pile group at Treasure Island test site

Full-Scale Field Test on a Pile Group in Clay

Full-scale load tests were conducted by Rollins et al. [42] on a single pile and a 9-group of driven piles (i.e., 3×3) with an S/D ratio of 3. The test piles were 9.1 m long, steel closed-end pipes with a 0.324 outer diameter, and 0.305 m inner diameter, installed into a stratified soil system characterized as soft to medium stiff clays and sands. The steel elastic modulus of 200 GPa was used. Both foundations were in a condition of free-head, and the site investigation provided two sets of soil properties (i.e., a detailed profile and a conservative one).

The present analysis adopts the conservative profile (Table 7) for practical purposes. For sand layers, the elastic modulus was calculated from the SPT blow count, N_{60} , using Equations. 13 to 15, and the average value was used (Table 7). For clay layers, the elastic modulus was defined as $500c_u$ [47, 48]. The R_f was set to 0.9 for the analysis of single pile. For the front row, middle row, and overall group analysis, R_f was set to 1.0 to capture the greater nonlinear behavior exhibited by the pile group.

	Soil Layer	Soil Layer $c_n (kN/m^2) \phi^o$			A.	(I-N/3)	E (MD~)	
No.	Thickness (m)	Type	$c_u(\kappa N/m^2)$	ϕ^o N_{60}		$\gamma'(kN/m^3)$	$E_s(MPa)$	
1	0.0 - 3.0	Clay	47.5	0.0	-	10.0	23.750	
2	3.0 - 4.8	Sand	0.0	36	30	10.0	82.786	
3	4.8 - 6.5	Clay	47.5	0.0	-	10.0	23.750	
4	6.5 - 7.5	Sand	0.0	36	30	10.0	82.786	

Table 7. Properties of the soil stratums [42]

The predicted lateral load-displacement curves for both the isolated pile and the group, illustrated in Figure 14, align well with the experimentally recorded data. The model produced an f_m value of 0.5 for the group, a result that corresponds closely to the value of 0.47 derived empirically by Rollins et al. [42].

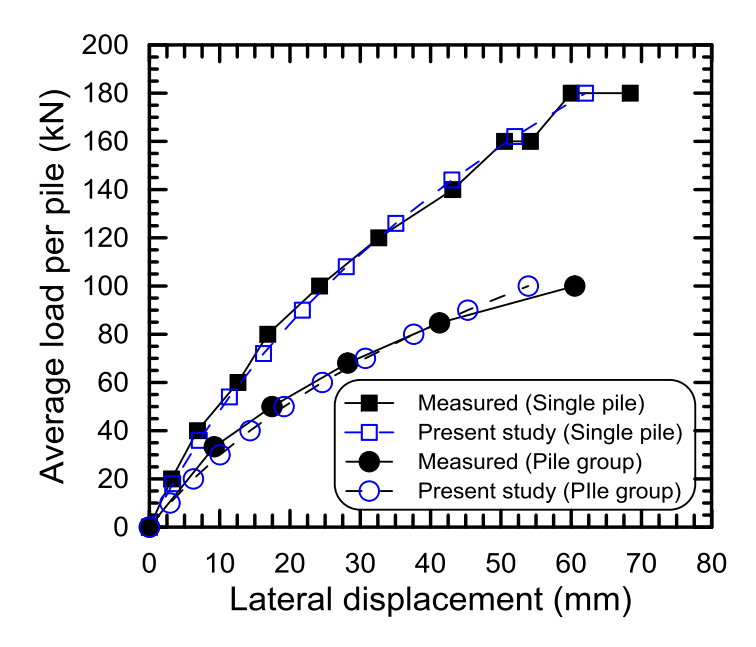


Figure 14. Measured and predicted lateral load-displacement curves of single pile and pile group in a multi-layered soil deposit (Rollins et al. [42])

A strong correlation is evident in Figure 15 between the measured and predictands load-displacement behavior for each row (i.e., front, middle, back). The analysis generated f_m values of 0.7 for the front row, 0.46 for the middle row, and 0.39 for the back row. These computed values show general consistency with the multipliers of 0.6, 0.38, and 0.43 reported by Rollins et al. [42], with one notable discrepancy: their published value for the back row (0.43) is higher than that for the middle row (0.38), a trend that is inverted in the results of the current program.

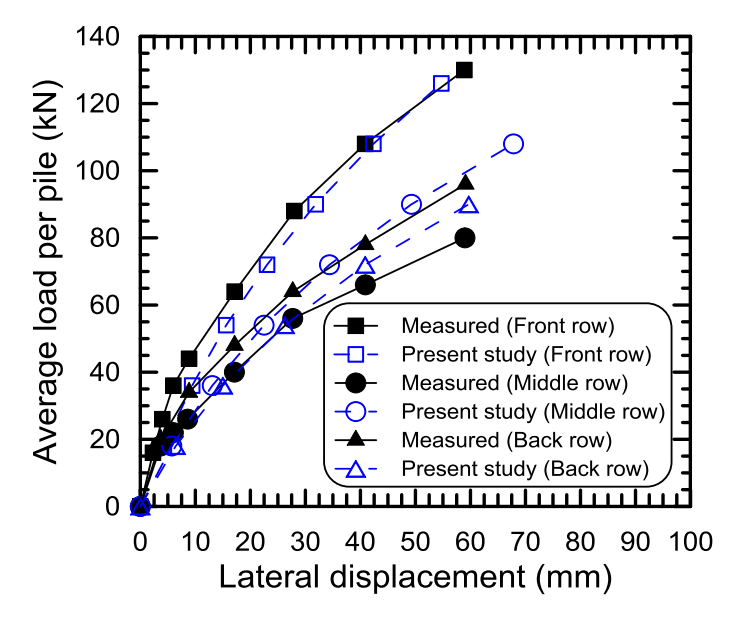


Figure 15. Measured and predicted lateral load-displacement curves for the front, middle, and back rows of the pile group in a multi-layered soil deposit (Rollins et al. [42])

Figure 16 compares the experimental and predicted moment distributions for a single pile at lateral loads of 53.6 kN and 97.9 kN. The model demonstrates strong agreement with field data at 53.6 kN, accurately capturing the value and depth of the maximum moment. At a higher load of 97.9 kN, the analysis provides a conservative prediction, overestimating the peak moment and placing its location slightly deeper than observed.

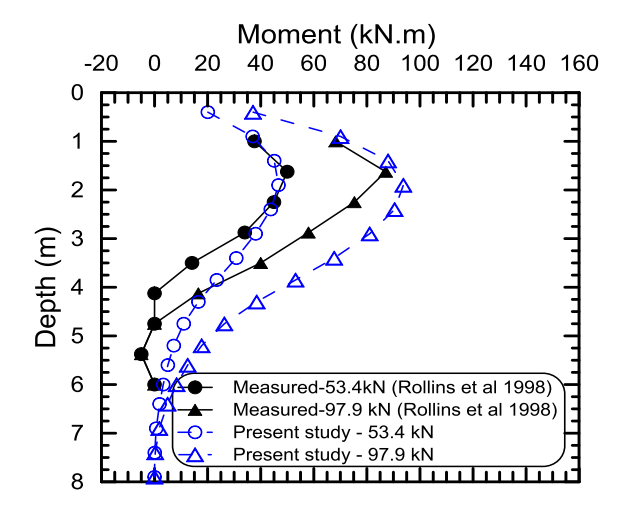


Figure 16. Measured versus computed bending moments for the single pile in a multi-layered soil deposit (Rollins et al. [42])

4. Parametric Study

A common approach for increasing the resistance to the laterally loaded piles in weak soil (e.g., soft clay and loose sand) is to employ ground improvement techniques on the upper layer of the weak soil. Among these techniques, the excavation and replacement of weak material with a compacted sand layer offers a particularly simple and economical solution. The impact of soil replacement on the lateral response of a single pile is examined through a parametric study, with the geometrical and material properties of the finite element model provided in Figure 17.

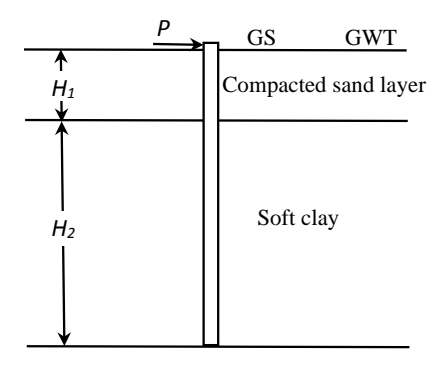


Figure 17. Replacement of the upper layer of soft clay with a compacted sand layer

As detailed in Table 8, the soft clay and compacted sand layers have markedly different geotechnical properties. The numerical model represents a 20 m pile length, a 0.5 m diameter, and elastic modulus of 21,000 MPa. The R_f is considered 0.95 across all studied cases.

Table 8. The properties of the compacted sand layer and soft clay for the parametric study

Item	Compacted sand layer	Soft clay
Thickness	0.0, 0.5, 1.0, 1.5, 2.0, 2.5	20.0, 19.5, 19.0, 18.5, 18.0, 17.5
Effective unit weight (kN/m ³)	10	8.0
Cohesion (kN/m^2)	-	30
Angle of internal friction (Degrees)	35	-
Modulus of elasticity (MPa)	20, 30, 40, 50, 60	9

4.1. Effect of the Sand Layer Thickness

To investigate the impact of the sand layer's thickness on lateral pile behavior. The thickness was systematically varied from 0 to 2.5 meters, corresponding to a range of 0 to 5 pile diameters (D = 0.5m), to assess its impact on the pile's behavior. The improvement in performance is quantified using two reduction factors, R_w and R_m . These factors are calculated as follows:

$$R_{w} = \frac{w_{o} - w}{w_{o}}$$

$$R_{m} = \frac{M_{o} - M}{M_{o}}$$

$$\tag{17}$$

$$R_m = \frac{M_o - M}{M_o} \tag{17}$$

where R_w and R_m are the reduction factors quantify the improvement in ground surface displacement, w, and maximum moment, M, respectively, w_o and M_o are the displacement and maximum moment for the untreated case

Figures 18 and 19 depict the load-displacement and load-maximum moment curves, respectively, demonstrating that increasing the sand layer thickness effectively reduces both displacement and maximum moment. These findings align with previous numerical studies on piles in stratified sand-clay profiles [19] and investigations into soil improvement techniques for lateral capacity [71].

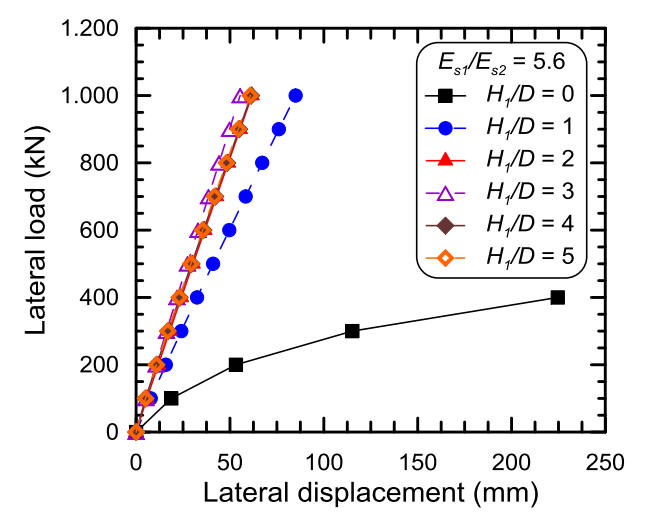


Figure 18. Effect of sand layer thickness on the load-displacement response (case of $E_{s1}/E_{s2}=5.6$)

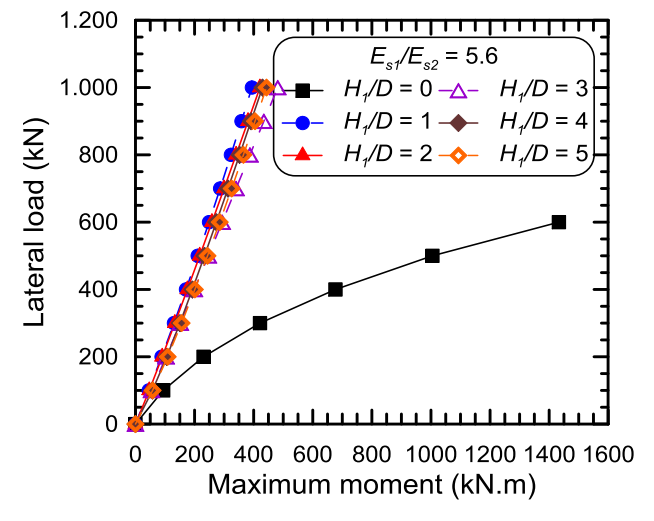


Figure 19. Impact of sand layer thickness on the lateral load maximum moment curve (case of $E_{s1}/E_{s2}=5.6$)

The optimum compacted sand layer thickness was determined by analyzing the relationship between the normalized thickness, H_1/D , and the reduction factors R_w and R_m . These relationships, plotted for different lateral load magnitudes, are presented in Figures 20 and 21.

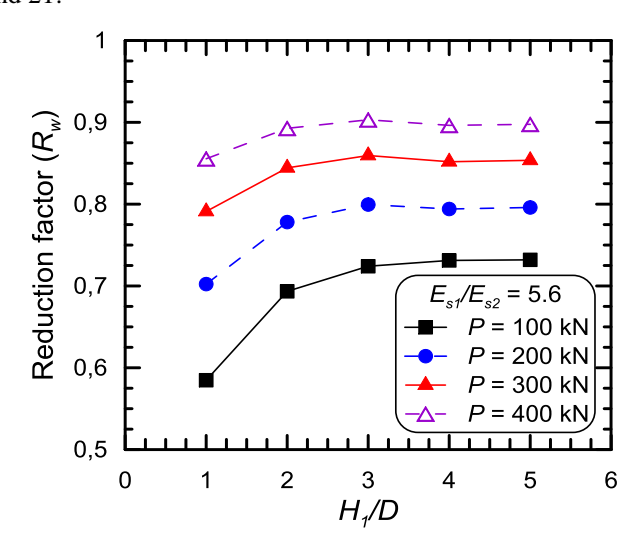


Figure 20. Impact of sand layer thickness on the reduction factor of the displacement at the ground at different lateral loads

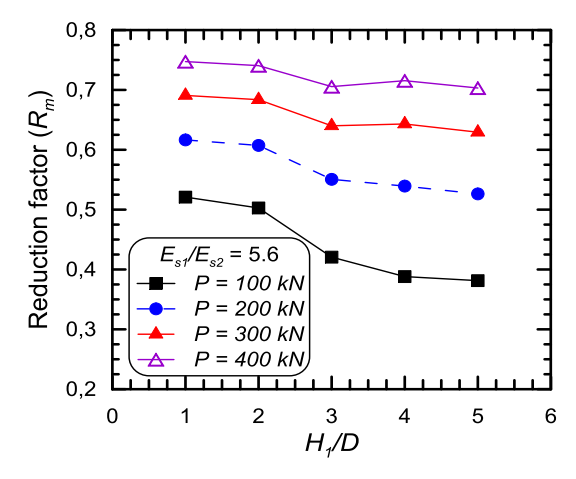


Figure 21. Impact of sand layer thickness on the reduction factor of the maximum moment in the pile at different lateral loads

The relationship between sand stratum depth and lateral pile capacity at displacements of 0.05D and 0.1D is illustrated in Figure 22.

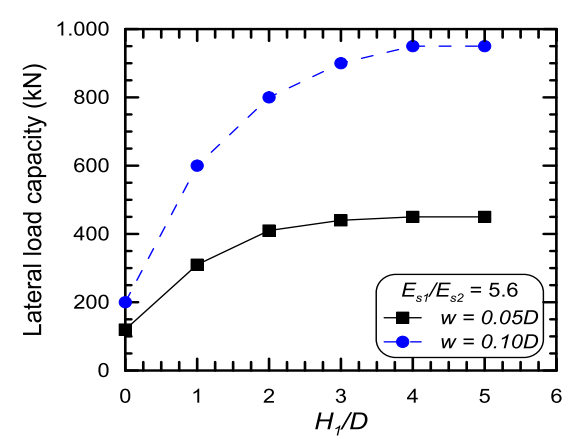


Figure 22. Effect of sand layer thickness on the lateral capacity of the pile at lateral displacements of 0.05D and 0.1D

Analysis of Figures 20 through 22 reveals the following key trends: (1) the displacement reduction factor, R_w , increases with both sand layer thickness and lateral load (Figure 20), (2) the moment reduction factor, R_m , decreases with sand layer thickness but increases with lateral load (Figure 21), (3) the lateral capacity at displacements of 0.05D and 0.1D increases with sand layer thickness (Figure 22), and (4) for practical purposes, an optimum sand layer thickness of 3D is identified. Beyond this depth, the rates of increase for R_w and lateral capacity, and the rate of decrease for R_m , become negligible, indicating diminishing returns on further investment.

Figures 23 and 24 depict the nonlinear increase in the reduction factors R_w and R_m with lateral load for various sand layer thicknesses. At a low load (P = 100 kN), R_w ranges from 0.58 to 0.73 and R_m from 0.38 to 0.53. These values approach 0.98 and 0.90, respectively, at a high load (P = 1000 kN), indicating a convergence in pile performance. The results confirm that the benefit of increasing the layer thickness beyond 3D is negligible, thereby validating this value as the practical optimum.

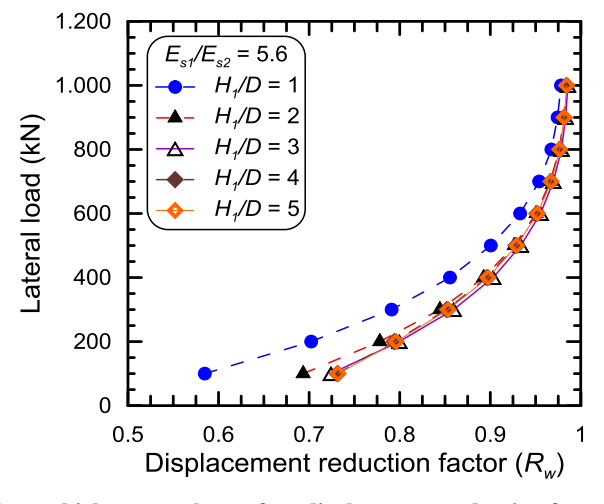


Figure 23. Effect of sand layer thickness on the surface displacement reduction factor at different lateral loads

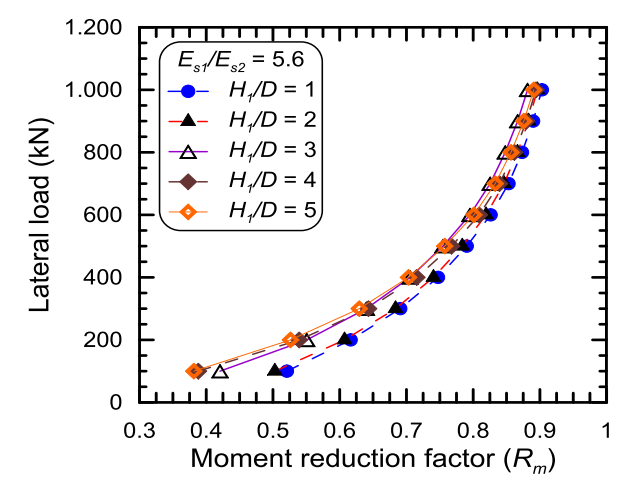


Figure 24. Effect of sand layer thickness on the maximum moment reduction factor at different lateral loads

4.2. Effect of the Sand Layer Stiffness

To investigate the impact of sand stratum's stiffness, the elasticity modulus of the sand stratum, E_{s1} , was changed from 20 MPa to 60 MPa, while its thickness was held constant at the previously identified optimum of 3D. All other geotechnical and structural parameters for the soil layers (Table 8) and the pile were kept unchanged from the prior investigation.

The impact of the sand stratum's stiffness on the pile response is presented in Figures 25 and 26. The results indicate a consistent trend: higher layer stiffness causes a significant reduce in the displacement and a more moderate reduction in maximum bending moment. This suggests that soil improvement via stiffening is more effective at enhancing serviceability (controlling displacement) than at reducing structural demand on the pile (bending moment).

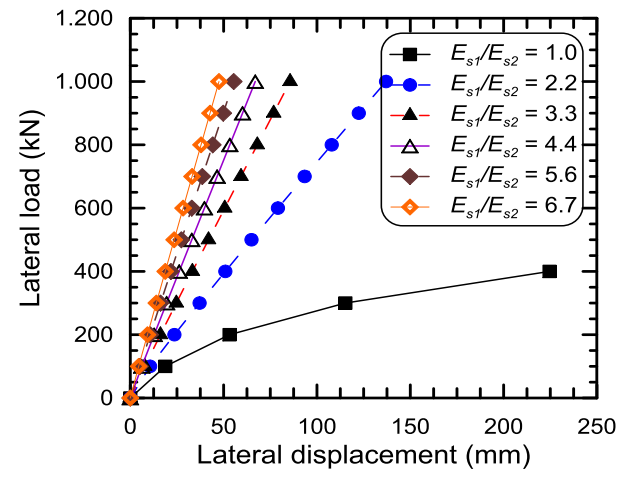


Figure 25. Effect of sand layer stiffness on the lateral load-displacement response (case of $H_1 = 3D$)

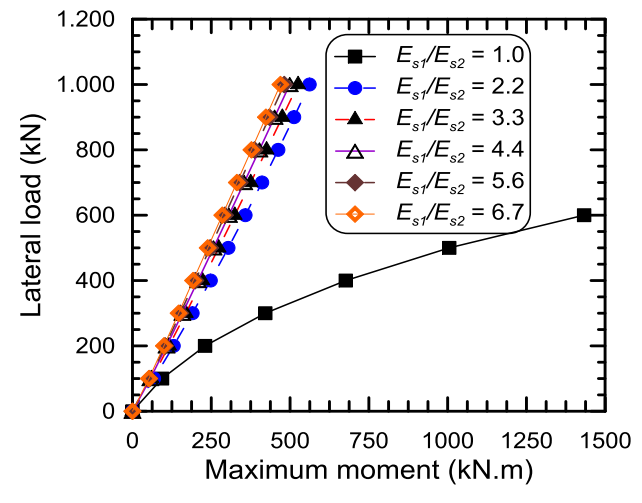


Figure 26. Impact of sand layer stiffness on the lateral load-maximum moment curve for the case of $H_1 = 3D$

Figures 27 and 28 plot the reduction factors, R_w and R_m , against the stiffness ratio, E_{s1}/E_{s2} , for various lateral loads. The key trends are: (1) both R_w and R_m increase with higher stiffness ratios and lateral loads. For instance, at P=300 kN, R_w rises from 0.68 to 0.79 and R_m from 0.55 to 0.6 as E_{s1}/E_{s2} ratio changes from 2.2 to 3.3, (2) the rate of increase for R_w is consistently greater than for R_m , (3) the rate of increase for both factors diminish at higher stiffness ratios, indicating diminishing returns, and (4) an optimum stiffness ratio of 5.6 is identified. Beyond this point, improvements are marginal, increasing the ratio from 5.6 to 6.7 at P=300 kN only raises R_w from 0.86 to 0.88 and R_m from 0.64 to 0.65.

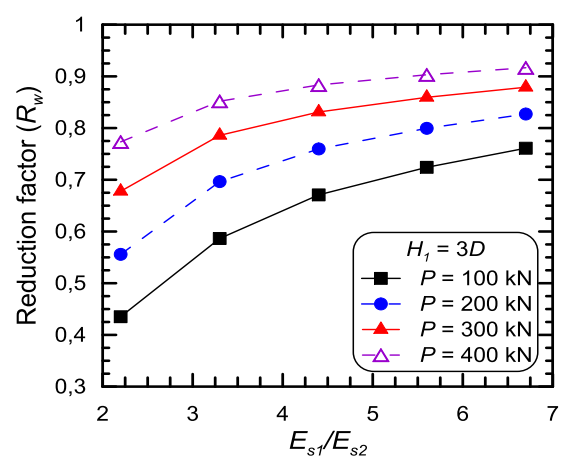


Figure 27. Impact of sand layer stiffness on the reduction factor of the lateral displacement at the ground surface at different lateral loads

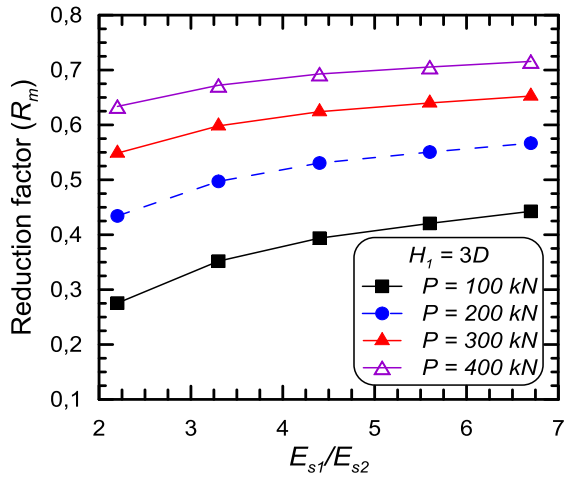


Figure 28. Effect of sand layer stiffness on the reduction factor of the maximum moment in the pile at different lateral loads

Figures 29 and 30 depict that the reduction factors R_w and R_m grow nonlinearly with lateral load at different stiffness ratios, E_{s1}/E_{s2} . The figures highlight a critical contrast: a large dispersion of values at low loads (e.g., P=100 kN) and a strong convergence at high loads (e.g., P=1000 kN). This convergence, alongside the overlapping curves for ratios beyond 5.6, confirms this value as the effective optimum for the stiffness ratio.

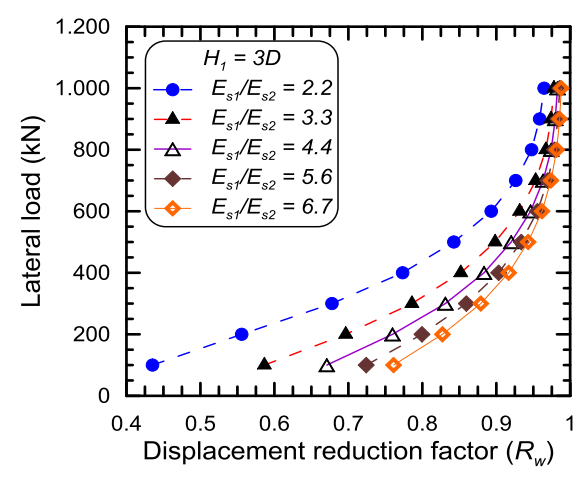


Figure 29. Effect of sand layer stiffness on the maximum moment reduction factor at different lateral loads

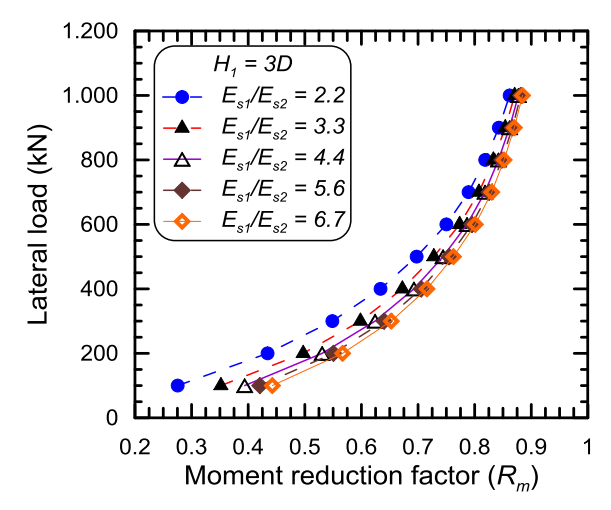


Figure 30. Effect of sand layer stiffness on the maximum moment reduction factor at different lateral loads

5. Conclusions

This study details an analytical procedure for the nonlinear analysis of isolated pile and pile groups under lateral loads in multi-layered, heterogeneous soil deposits. The proposed procedure integrates the FEM, the p-y technique, and the p-multiplier concept, implemented within an original computational code. Hyperbolic p-y curves, following the Duncan & Chang [44] model, are defined by three parameters: initial tangent stiffness, limiting soil resistance, and a curvature parameter controlling nonlinearity. A new equation for the p-multiplier, f_m , is introduced and validated for group pile analysis. The proposed program's accuracy is checked through comparisons with 3D FEA and field loading tests on both isolated piles and pile groups in various soil deposits. The proposed program facilitated a parametric study to quantify the effect of ground improvement technique, achieved by replacing the upper soft clay with compacted sand, on the performance of an isolated pile

The findings of this study support the following conclusions:

- The proposed program accurately predicts the behavior of laterally loaded individual piles and pile groups embedded in diverse, multi-layered soil deposits. Validation against 3D FEA and field load tests confirms that the model's predictions of load-displacement behavior exhibit a close correlation with both numerical results and experimentally measured data.
- The three-parameter hyperbolic Duncan-Chang model provides a satisfactorily accurate representation of p-y
 curves for both sand and clay soils. This formulation effectively captures the nonlinear soil response essential for
 the analysis of piles that are laterally loaded.
- Validation through comparison with field loading tests and existing methods confirms the applicability of the suggested p-multiplier, f_m, equation for small pile diameter (≤1.0 m). Further investigation is necessary to determine its suitability for larger-diameter piles, such as monopiles.
- The replacement of the upper soft clay layer with compacted sand significantly enhances the lateral performance of piles, markedly reducing both ground surface displacement and maximum moment. The efficacy of this improvement is quantified by reduction factors R_w and R_m which increase nonlinearly with lateral loads across all tested sand layer thicknesses and stiffness values. For the cases studied, the optimal design parameters were determined to be a sand layer thickness of 3D and a stiffness of 5.6 times that of the native soft clay.

The main benefits of the current program are that it offers a practical way to get precise answers with comparatively minimal input data, is computationally more cost-effective than the full 3D FEA, and is suitable in the preliminary design stage of single piles and pile groups loaded laterally. Despite obtaining satisfactory predictions, the current program needs more validation through comparisons with field measurements, 3D FEA, and previous studies, including results from existing programs such as LPILE. While the proposed program is robust for the preliminary design stage and parametric studies, its use is subject to important limitations. Advanced 3D FEA is recommended for more complex scenarios such as pile groups with inclined piles, large-diameter monopiles, sites of extreme spatial soil variability, and piles subjected to dynamic loads from earthquakes or wind.

6. Declarations

6.1. Author Contributions

Conceptualization, B.E. and A.A.; methodology, B.E., T.A., and A.A.; software, B.E.; validation, B.E., T.A., and A.A.; formal analysis, B.E.; investigation, B.E.; resources, T.A.; data curation, A.A.; writing—original draft preparation, A.A.; writing—review and editing, B.E.; visualization, T.A.; supervision, B.E. All authors have read and agreed to the published version of the manuscript.

6.2. Data Availability Statement

The data presented in this study are available upon request from the corresponding author.

6.3. Funding

The authors received no financial support for the research, authorship, and/or publication of this article.

6.4. Conflicts of Interest

The authors declare no conflict of interest.

7. References

- [1] Brown, D. A., & Shie, C. F. (1991). Some numerical experiments with a three dimensional finite element model of a laterally loaded pile. Computers and Geotechnics, 12(2), 149–162. doi:10.1016/0266-352X(91)90004-Y.
- [2] Hidayawanti, R., Latief, Y., & Gaspersz, V. (2024). Risk-Based Method-Technology Integration on Spun Pile Production for Product and Service Quality. Civil Engineering Journal, 10(11), 3683–3698. doi:10.28991/CEJ-2024-010-11-015.
- [3] Gui, M. W., & Alebachew, A. A. (2025). Numerical investigation of laterally loaded pile groups at the crest of slopes. Scientific Reports, 15(1), 22670. doi:10.1038/s41598-025-07715-x.
- [4] Elsiragy, M., Azzam, W., & Kassem, E. M. (2025). Experimental and Numerical Study of Enlarged-Head Monopile Under Lateral Load in Soft Clay. Civil Engineering Journal (Iran), 11(2), 453–471. doi:10.28991/CEJ-2025-011-02-04.
- [5] Poulos, H. G. & Davis, E. H. (1980). Pile foundation analysis and design (1st Ed.), John Wiley and Sons, New York, United States.
- [6] Matlock, H., & Reese, L. C. (1960). Generalized Solutions for Laterally Loaded Piles. Journal of the Soil Mechanics and Foundations Division, 86(5), 63–92. doi:10.1061/jsfeaq.0000303.
- [7] Reese, L. C., Cox, W. R., & Koop, F. D. (1974). Analysis of Laterally Loaded Piles in Sand. Offshore Technology Conference. doi:10.4043/2080-ms.
- [8] Reese, L. C., & Welch, R. C. (1975). Lateral Loading of Deep Foundations in Stiff Clay. Journal of the Geotechnical Engineering Division, 101(7), 633–649. doi:10.1061/ajgeb6.0000177.
- [9] Reese, L. C., Wang, S. T., Isenhower, W. M., Arrellaga, J. A., & Hendrix, J. (2000). A program for the analysis of piles and drilled shafts under lateral loads. LPILE version, 4, Ensoft, Inc., Austin, United States.
- [10] Ashford, S. A., & Juirnarongrit, T. (2003). Evaluation of Pile Diameter Effect on Initial Modulus of Subgrade Reaction. Journal of Geotechnical and Geoenvironmental Engineering, 129(3), 234–242. doi:10.1061/(asce)1090-0241(2003)129:3(234).
- [11] Castelli, F., & Maugeri, M. (2009). Simplified Approach for the Seismic Response of a Pile Foundation. Journal of Geotechnical and Geoenvironmental Engineering, 135(10), 1440–1451. doi:10.1061/(asce)gt.1943-5606.0000107.
- [12] Alver, O., & Eseller-Bayat, E. E. (2024). A new p-y model for soil-pile interaction analyses in cohesionless soils under monotonic loading. Soils and Foundations, 64(2), 101441. doi:10.1016/j.sandf.2024.101441.
- [13] El Gendy, M. (2025). Analyzing laterally loaded piles in multi-layered cohesive soils: a hybrid beam on nonlinear Winkler foundation approach with case studies and parametric study. Discover Civil Engineering, 2(1), 1-34. doi:10.1007/s44290-025-00240-w.
- [14] Ashour, M., Norris, G., & Pilling, P. (1998). Lateral Loading of a Pile in Layered Soil Using the Strain Wedge Model. Journal of Geotechnical and Geoenvironmental Engineering, 124(4), 303–315. doi:10.1061/(asce)1090-0241(1998)124:4(303).
- [15] Ashour, M., & Norris, G. (2000). Modeling Lateral Soil-Pile Response Based on Soil-Pile Interaction. Journal of Geotechnical and Geoenvironmental Engineering, 126(5), 420–428. doi:10.1061/(asce)1090-0241(2000)126:5(420).
- [16] Ashour, M., Pilling, P., & Norris, G. (2004). Lateral Behavior of Pile Groups in Layered Soils. Journal of Geotechnical and Geoenvironmental Engineering, 130(6), 580–592. doi:10.1061/(asce)1090-0241(2004)130:6(580).
- [17] Reese, L. C., & Van Impe, W. F. (2010). Single Piles and Pile Groups Under Lateral Loading. CRC Press, London, United Kingdom. doi:10.1201/b17499.
- [18] API. (2014). Recommended Practice 2A-WSD- Planning, Designing, and Constructing Fixed Offshore Platforms Working Stress Design. American Petroleum Institute (API), Washington, united States.
- [19] AASHTO. (2000). Bridge design specifications. American Association of State Highway and Transportation Officials (AASHTO), Washington, United States.
- [20] Matlock, H. (1970). Correlation for Design of Laterally Loaded Piles in Soft Clay. Offshore Technology Conference. doi:10.4043/1204-ms.

- [21] Kim, Y., & Jeong, S. (2011). Analysis of soil resistance on laterally loaded piles based on 3D soil-pile interaction. Computers and Geotechnics, 38(2), 248–257. doi:10.1016/j.compgeo.2010.12.001.
- [22] Bhuiyan, F. M. (2022). Development of a New Load Analysis Tool and a Unified Py Method for Lateral Analysis of Large-Diameter Drilled Shafts Validated Using Load Tests. PhD Thesis, University of Nevada, Reno, United States.
- [23] Yang, K., & Liang, R. (2006). Numerical Solution for Laterally Loaded Piles in a Two-Layer Soil Profile. Journal of Geotechnical and Geoenvironmental Engineering, 132(11), 1436–1443. doi:10.1061/(asce)1090-0241(2006)132:11(1436).
- [24] Liam Finn, W. D., & Dowling, J. (2016). Modelling effects of pile diameter. Canadian Geotechnical Journal, 53(1), 173–178. doi:10.1139/cgj-2015-0119.
- [25] McVay, M. C., & Niraula, L. (2004). Development of PY curves for large diameter piles/drilled shafts in limestone for FBPIER. No. Final Report, University of Florida, Gainesville, United States.
- [26] Murchison, J. M., & O'Neill, M. W. (1984). Evaluation of p-y relationships in cohesionless soils, analysis and design of pile foundations. Proceedings of the Symposium in Conjunction with the ASCE National Convention, 1-5 October, 1984, San Francisco, United States.
- [27] Choi, J. I., Kim, M. M., & Brandenberg, S. J. (2015). Cyclic p-y Plasticity Model Applied to Pile Foundations in Sand. Journal of Geotechnical and Geoenvironmental Engineering, 141(5), 8216001. doi:10.1061/(asce)gt.1943-5606.0001261.
- [28] Rahmani, A., Taiebat, M., Finn, W. D. L., & Ventura, C. E. (2018). Evaluation of p-y springs for nonlinear static and seismic soil-pile interaction analysis under lateral loading. Soil Dynamics and Earthquake Engineering, 115, 438–447. doi:10.1016/j.soildyn.2018.07.049.
- [29] Wang, L., & Ishihara, T. (2022). New p-y model for seismic loading prediction of pile foundations in non-liquefiable and liquefiable soils considering modulus reduction and damping curves. Soils and Foundations, 62(5), 101201. doi:10.1016/j.sandf.2022.101201.
- [30] Georgiadis, M., Anagnostopoulos, C., & Saflekou, S. (1992). Centrifugal testing of laterally loaded piles in sand. Canadian Geotechnical Journal, 29(2), 208–216. doi:10.1139/t92-024.
- [31] Kondner, R. L. (1963). Hyperbolic Stress-Strain Response: Cohesive Soils. Journal of the Soil Mechanics and Foundations Division, 89(1), 115–143. doi:10.1061/jsfeaq.0000479.
- [32] Tak Kim, B., Kim, N.-K., Jin Lee, W., & Su Kim, Y. (2004). Experimental Load-Transfer Curves of Laterally Loaded Piles in Nak-Dong River Sand. Journal of Geotechnical and Geoenvironmental Engineering, 130(4), 416–425. doi:10.1061/(asce)1090-0241(2004)130:4(416).
- [33] Papadopoulou, M. C., & Comodromos, E. M. (2014). Explicit extension of the p-y method to pile groups in sandy soils. Acta Geotechnica, 9(3), 485–497. doi:10.1007/s11440-013-0274-z.
- [34] Lim, H., Jeong, S., & Chung, M. (2018). Analysis of Soil Resistance on Laterally Loaded Offshore Piles in Inchon Marine Clay. Innovations in Geotechnical Engineering, 147–159. doi:10.1061/9780784481639.009.
- [35] Zhou, P., Zhou, H., Liu, H., Li, X., Ding, X., & Wang, Z. (2020). Analysis of lateral response of existing single pile caused by penetration of adjacent pile in undrained clay. Computers and Geotechnics, 126, 103736. doi:10.1016/j.compgeo.2020.103736.
- [36] Lu, W., Kaynia, A. M., & Zhang, G. (2021). Centrifuge study of p-y curves for vertical-horizontal static loading of piles in sand. International Journal of Physical Modelling in Geotechnics, 21(6), 275–294. doi:10.1680/jphmg.19.00030.
- [37] Amar Bouzid, D. (2021). Analytical Quantification of Ultimate Resistance for Sand Flowing Horizontally around Monopile: New p-y Curve Formulation. International Journal of Geomechanics, 21(3), 4021007. doi:10.1061/(asce)gm.1943-5622.0001927.
- [38] Liang, R. Y., Shatnawi, E. S., & Nusairat, J. (2007). Hyperbolic P-Y criterion for cohesive soils. Jordan Journal of Civil Engineering, 1(1), 38–58.
- [39] Brown, D. A., Morrison, C., & Reese, L. C. (1988). Lateral load behavior of pile group in sand. Journal of Geotechnical Engineering, 114(11), 1261–1276. doi:10.1061/(ASCE)0733-9410(1988)114:11(1261).
- [40] Hoit, M., Hays, C., & McVay, M. (1997). The Florida Pier Analysis Program Methods and Models for Pier Analysis and Design. Transportation Research Record: Journal of the Transportation Research Board, 1569(1), 1–7. doi:10.3141/1569-01.
- [41] Ruesta, P. F., & Townsend, F. C. (1997). Evaluation of Laterally Loaded Pile Group at Roosevelt Bridge. Journal of Geotechnical and Geoenvironmental Engineering, 123(12), 1153–1161. doi:10.1061/(asce)1090-0241(1997)123:12(1153).
- [42] Rollins, K. M., Peterson, K. T., & Weaver, T. J. (1998). Lateral Load Behavior of Full-Scale Pile Group in Clay. Journal of Geotechnical and Geoenvironmental Engineering, 124(6), 468–478. doi:10.1061/(asce)1090-0241(1998)124:6(468).
- [43] Zhang, X. (1999). Comparison of lateral group effect between bored and PC driven pile groups in sand. Master Thesis, University of Houston, Houston, United States.

- [44] Duncan, J. M., & Chang, C.-Y. (1970). Nonlinear Analysis of Stress and Strain in Soils. Journal of the Soil Mechanics and Foundations Division, 96(5), 1629–1653. doi:10.1061/jsfeaq.0001458.
- [45] Poulos, H. G. (1989). Pile behaviour theory and application. Geotechnique, 39(3), 365–415. doi:10.1680/geot.1989.39.3.365.
- [46] Yu, Y., Shen, M., & Hsein Juang, C. (2019). Assessing Initial Stiffness Models for Laterally Loaded Piles in Undrained Clay: Robust Design Perspective. Journal of Geotechnical and Geoenvironmental Engineering, 145(10), 4019073. doi:10.1061/(asce)gt.1943-5606.0002074.
- [47] Callanan, J. F. (1984). Evaluation of procedures for predicting foundation uplift movements. Cornell University, Report EL-4107 Electric Power Research Institute, Palo Alto, California, United States.
- [48] Bowles, J.E. (1996) Foundation Analysis and Design (5th Ed.). McGraw-Hill Companies, Inc., New York, United States.
- [49] Kulhawy, F. H., & Mayne, P. W. (1990). Manual on estimating soil properties for foundation design. No. EPRI-EL-6800, Electric Power Research Inst., Palo Alto, United States.
- [50] Duncan, J. M., & Bursey, A. (2013). Soil Modulus Correlations. Foundation Engineering in the Face of Uncertainty, 321–336. doi:10.1061/9780784412763.026.
- [51] Wagh, J. D., & Bambole, A. N. (2024). Improved correlation of soil modulus with SPT N values. Open Engineering, 14(1), 1–17. doi:10.1515/eng-2024-0046.
- [52] Jeong, S., Kim, Y., & Kim, J. (2011). Influence on lateral rigidity of offshore piles using proposed p-y curves. Ocean Engineering, 38(2–3), 397–408. doi:10.1016/j.oceaneng.2010.11.007.
- [53] Briaud, J.-L., Smith, T., & Meyer, B. (1984). Laterally Loaded Piles and the Pressuremeter: Comparison of Existing Methods. Laterally Loaded Deep Foundations: Analysis and Performance, 97–111, ASTM International, Pennsylvania, United States. doi:10.1520/stp36815s.
- [54] Zhang, L. M., McVay, M. C., Han, S. J., Lai, P. W., & Gardner, R. (2002). Effects of dead loads on the lateral response of battered pile groups. Canadian Geotechnical Journal, 39(3), 561–575. doi:10.1139/t02-008.
- [55] McVay, M. C., Shang, T. I., & Casper, R. (1996). Centrifuge testing of fixed-head laterally loaded battered and plumb pile groups in sand. Geotechnical Testing Journal, 19(1), 41–50. doi:10.1520/gtj11406j.
- [56] Rollins, K. M., Olsen, R. J., Egbert, J. J., Jensen, D. H., Olsen, K. G., & Garrett, B. H. (2006). Pile Spacing Effects on Lateral Pile Group Behavior: Load Tests. Journal of Geotechnical and Geoenvironmental Engineering, 132(10), 1262–1271. doi:10.1061/(asce)1090-0241(2006)132:10(1262).
- [57] Cox, W., Dixon, D., & Murphy, B. (1984). Lateral-Load Tests on 25.4-mm (1-in.) Diameter Piles in Very Soft Clay in Side-by-Side and In-Line Groups. Laterally Loaded Deep Foundations: Analysis and Performance, 122–139, ASTM International, Pennsylvania, United States. doi:10.1520/stp36817s.
- [58] Myint Lwin, M. (1999). Why the AASHTO load and resistance factor design specifications?. Transportation Research Record, 1688(1), 173-176. doi:10.3141/1688-20.
- [59] Walsh, K. D., Fréchette, D. N., Houston, W. N., & Houston, S. L. (2000). State of the practice for design of groups of laterally loaded drilled shafts. Transportation Research Record, 2000(1736), 33–40. doi:10.3141/1736-05.
- [60] Brown, D. A., Reese, L. C., & O'Neill, M. W. (1987). Cyclic lateral loading of a large-scale pile group. Journal of Geotechnical Engineering, 113(11), 1326–1343. doi:10.1061/(ASCE)0733-9410(1987)113:11(1326).
- [61] Mokwa, R. L., & Duncan, J. M. (2001). Laterally loaded pile group effects and p-y multipliers. Foundations and ground improvement, American Society of Civil Engineers (ASCE), Reston, United States.
- [62] FEMA P-751. (2012). 2009 NEHRP Recommended Seismic Provisions: Design Examples. Federal Emergency Management Agency (FEMA), Washington, United States.
- [63] Barker, R. M., & Puckett, J. A. (1987). Design of highway bridges based on AASHTO LRFD bridge design specifications. John Wiley & Sons, New York, United States.
- [64] Gupta, B. K., & Basu, D. (2020). Nonlinear solutions for laterally loaded piles. Canadian Geotechnical Journal, 57(10), 1566–1580. doi:10.1139/cgj-2019-0341.
- [65] Comodromos, E. M., & Pitilakis, K. D. (2005). Response evaluation for horizontally loaded fixed-head pile groups using 3-D non-linear analysis. International Journal for Numerical and Analytical Methods in Geomechanics, 29(6), 597–625. doi:10.1002/nag.428.
- [66] Reese, L. C. (1986). Behavior of piles and pile groups under lateral load. No. FHWA-RD-85-106, Department of Transportation, Federal Highway Administration, Washington, United States.

- [67] Wu, D., Broms, B. B., & Choa, V. (1998). Design of laterally loaded piles in cohesive soils using p-y curves. Soils and Foundations, 38(2), 17–26. doi:10.3208/sandf.38.2_17.
- [68] Guo, W. D. (2013). Simple Model for Nonlinear Response of 52 Laterally Loaded Piles. Journal of Geotechnical and Geoenvironmental Engineering, 139(2), 234–252. doi:10.1061/(asce)gt.1943-5606.0000726.
- [69] Rollins, K. M., Lane, J. D., & Gerber, T. M. (2005). Measured and Computed Lateral Response of a Pile Group in Sand. Journal of Geotechnical and Geoenvironmental Engineering, 131(1), 103–114. doi:10.1061/(asce)1090-0241(2005)131:1(103).
- [70] Bolton, M. D. (1986). The strength and dilatancy of sands. Geotechnique, 36(1), 65–78. doi:10.1680/geot.1986.36.1.65.
- [71] Eltaweila, S., Shahien, M. M., Nasr, A. M., & Farouk, A. (2021). Effect of Soil Improvement Techniques on Increasing the Lateral Resistance of Single Piles in Soft Clay (Numerical Investigation). Geotechnical and Geological Engineering, 39(6), 4059–4070. doi:10.1007/s10706-020-01534-9.